JOURNAL OF MATERIALS SCIENCE 33 (1998) 749–754

The effect of rare-earth oxides on the crystallization of $CaO–Al_2O_3–SiO_2$ glasses

M. UO*, H. SETO‡, K. MORITA, H. INOUE A. MAKISHIMA
Department of Materials Science, Faculty of Engineering, University of Tokyo 7-3-1 Hongo, Bunkyo-ku, Tokyo 113, Japan

$CaO–Al_2O_3–SiO_2–La_2O_3–Nd_2O_3$ glass was prepared and their physical properties, such as density, glass transition temperature and crystallization temperature, were measured. The heat treatment of these glasses precipitated $Ca_2La_8(SiO_4)_6O_2$ oxyapatite (CLS) crystal for $20CaO–10Al_2O_3–60SiO_2–10La_2O_3$ (mol %) glass and $Ca_2Nd_8(SiO_4)_6O_2$ oxyapatite (CNS) crystal was precipitated with Nd_2O_3 substitution. Crystallization of these glasses was observed at the surface and internally within the samples. The spherical and stick-like crystals were observed throughout the bulk of the glasses and the surface crystal layer of oxyapatite crystals were strongly oriented along the *c*-axis. The apparent activation energies of crystal growth were estimated as 360 kJ mol^{-1}. © *1998 Chapman & Hall*

1. Introduction

Machinable glass ceramics, which can be machined using equipment for the machining of metals, are useful as heat-resistant materials, electrical insulation, and chemically durable materials. Usually, machinable glass ceramics contain mica, and show high machinability because of the cleavage of precipitated mica in the glass [1, 2]. However, these glass ceramics show a lower mechanical strength compared to ordinary glasses.

The preparation and properties of machinable glass ceramics derived from yttria-containing calcium aluminosilicate glasses have been reported previously [3–5]. In this glass, tubular and hexagonal prism-like $Ca_4Y_6O(SiO_4)_6$ oxyapatite crystals were precipitated and the machinability of this glass was obtained from the precipitated crystals. The machinability was affected by the conditions of the precipitated oxyapatite crystals.

In this study, lanthanum and neodium oxide containing calcium aluminosilicate glasses were prepared and the effects of rare-earth oxide on crystallization properties were investigated.

2. Experimental procedure

The compositions of prepared glasses are shown in Table I. In this experiment, concentrations of CaO, Al_2O_3 and SiO_2 were fixed at 20, 10 and 60 mol %, respectively, and those of La_2O_3 and Nd_2O_3 were varied between 0 and 10 mol %. Reagent-grade chemicals of $CaCO_3$, Al_2O_3, SiO_2, Y_2O_3, La_2O_3 and Nd_2O_3 were mixed and the mixture was melted in a Pt–10%Rh crucible at 1600 °C for 4 h in air and quenched. The quenched glass was crushed and remelted at 1600 °C for 4 h in air to achieve homogeneity. After melting, the melt was cast into a graphite mould heated at 800 °C and cooled to room temperature. Differential thermal analysis (DTA; TAS-100, Rigaku Denki, Tokyo, Japan) was performed on these glass samples to determine glass transition temperature and crystallization temperature. Densities were obtained by the Archimedes method using kerosene.

The obtained glasses were cut into disc form (3 mm thick, 20 mm diameter) and the surfaces were polished. These glass discs were heat treated to promote the crystallization. During the heat treatment, samples were buried in ZrO_2 powder to ensure homogeneity of the heat-treatment temperature.

The precipitated crystals were observed by polarizing microscope and their sizes were estimated. The crystal phases were determined by powder X-ray diffraction and micro X-ray diffraction (Model MXP^{18}, Mac Science, Tokyo, Japan).

3. Results and discussions

3.1. Properties of glasses

The densities, glass transition temperature, T_g, and crystallization temperature, T_x, were estimated as shown in Table II. The densities of these glasses were 3.48–3.55 g cm^{-3} and increased with increasing Nd_2O_3 concentration. T_g was not affected by the glass composition and T_x was slightly decreased with the addition of Nd_2O_3. In this investigation, heat-treatment temperatures were varied in the range 900–1000 °C.

* *Present address*: Department of Dental Materials and Engineering, School of Dentistry, Hokkaido University, North 13, West 7, Kita-ku, Sapporo-shi 060, Japan.
‡ *Present address*: Nippon Sheet Glass, Central Research Institute.

TABLE I Compositions of rare-earth oxide containing CaO–Al_2O_3–SiO_2 glasses

Composition	CaO	Al_2O_3	SiO_2	La_2O_3	Nd_2O_3
L10	20	10	60	10	0
L8N2	20	10	60	8	2
L6N4	20	10	60	6	4
L5N5	20	10	60	5	5
L4N6	20	10	60	4	6
L2N8	20	10	60	2	8
N10	20	10	60	0	10

TABLE II Density, glass transition temperature, T_g, and crystallization temperature, T_x of prepared glasses

Composition	density (g/cm^3)	Tg (°C)	Tx (°C)
L10	3.480	793	1040
L8N2		794	1043
L6N4	3.507	795	1041
L5N5	3.516	795	1044
L4N6	3.521	797	1036
L2N8	3.532	794	1033
N10	3.554	796	1031

3.2. Surface crystallization

Firstly, the cross-sections of heat-treated samples were observed by polarizing microscope. Fig. 1 shows the cross-section of heat-treated samples (L10 and L5N5). As shown in Fig. 1, the crystallization occurred along the surface and inside the sample. X-ray diffraction measurement were carried out for these surface crystallized samples to determine the phases of the surface crystals. Fig. 2 shows the X-ray diffraction pattern of L5N5 and L10N0 sample shown in Fig. 1. In Fig. 2, peaks of diffraction patterns of L5N5 and L10N0 were assigned as $Ca_2Nd_8(SiO_4)_6O_2$ oxyapatite (CNS) and $Ca_2La_8(SiO_4)_6O_2$ oxyapatite (CLS), respectively. The strong diffraction from (002) and (004) surfaces of CLS and CNS oxyapatite crystals were observed in Fig. 2 and this shows that the surface crystals strongly oriented along the *c*-axis.

Fig. 3 shows the change in diffraction patterns of the L5N5 surface crystal with the depth from the surface. In this measurement, the surface crystal layer was removed by polishing and XRD patterns were measured on each 80 μm polishing. Up to 400 μm polishing, diffraction peaks from (002) and (004) reflections of CNS oxyapatite were observed.

The thickness of surface crystals was measured by optical microscopy at various temperatures between 945 and 1000 °C. Fig. 4a and b show the dependence of the thickness of the surface crystal and time of heat treatment of L10N0 and L5N5 samples, respectively. The thickness of the surface crystal linearly increased with respect to time of heat treatment and the neodium containing sample (L5N5) showed larger growth rate.

3.3 Internal crystallization

The shape of the internal crystals was characteristic of these glasses as shown in Fig. 5. In the L10 sample,

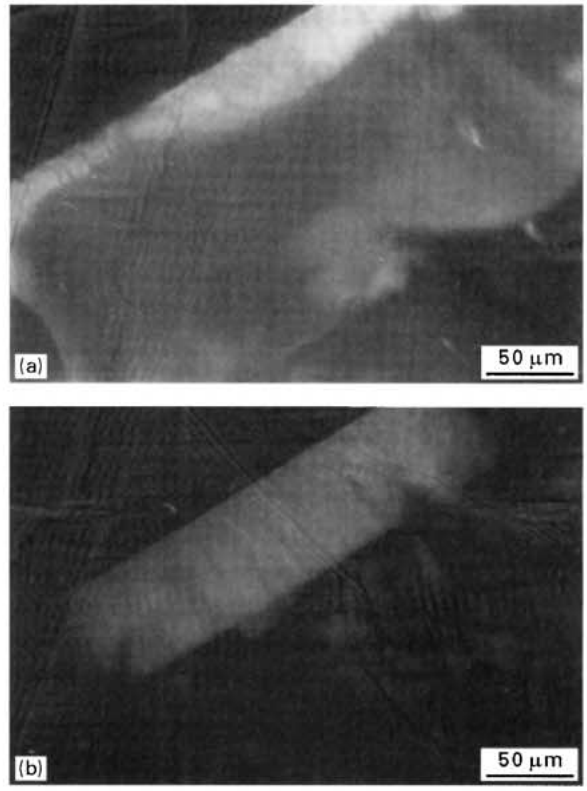

Figure 1 Surface crystals observed by polarizing microscopy. (a) L10 heat treated at 975 °C for 10 h. (b) L5N5 heat treated at 960 °C for 16 h.

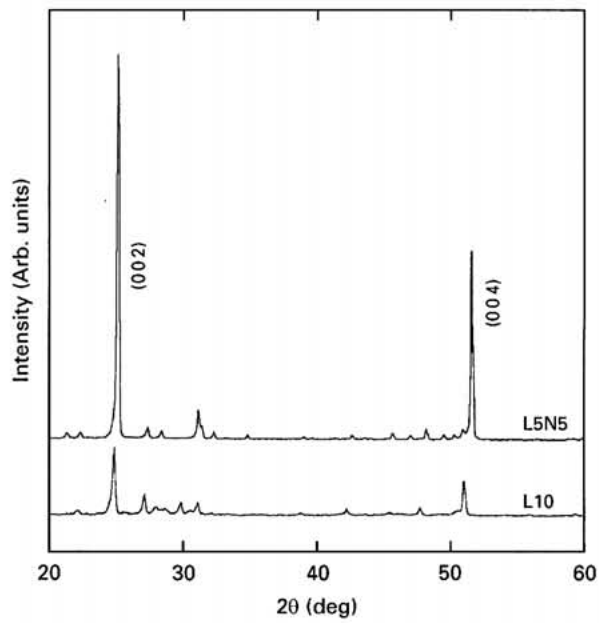

Figure 2 X-ray diffraction spectrum for crystallized L10 and L5N5 samples.

spherical and stick-shaped crystals were observed as in Fig. 5a and b. In the L5N5 sample, stick-shaped crystals were observed as in Fig. 5c.

The powder X-ray diffraction patterns of internal crystals were measured by removing surface crystal layers by polishing. Fig. 6 shows the change in XRD patterns by substitution of Nd_2O_3 for La_2O_3. In L10, most of the crystalline phase was CLS. The precipitation of CNS was observed on substitution of La_2O_3

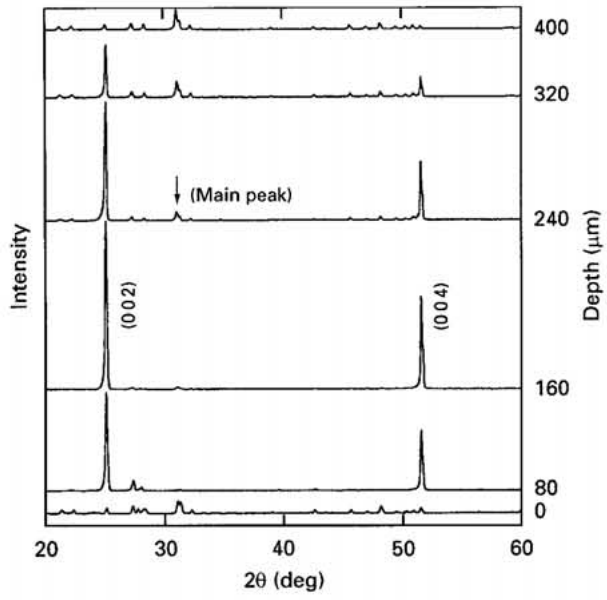

Figure 3 Change in XRD profiles of crystallized L5N5 sample with the depth from the surface (heat treated at 985 °C for 8 h).

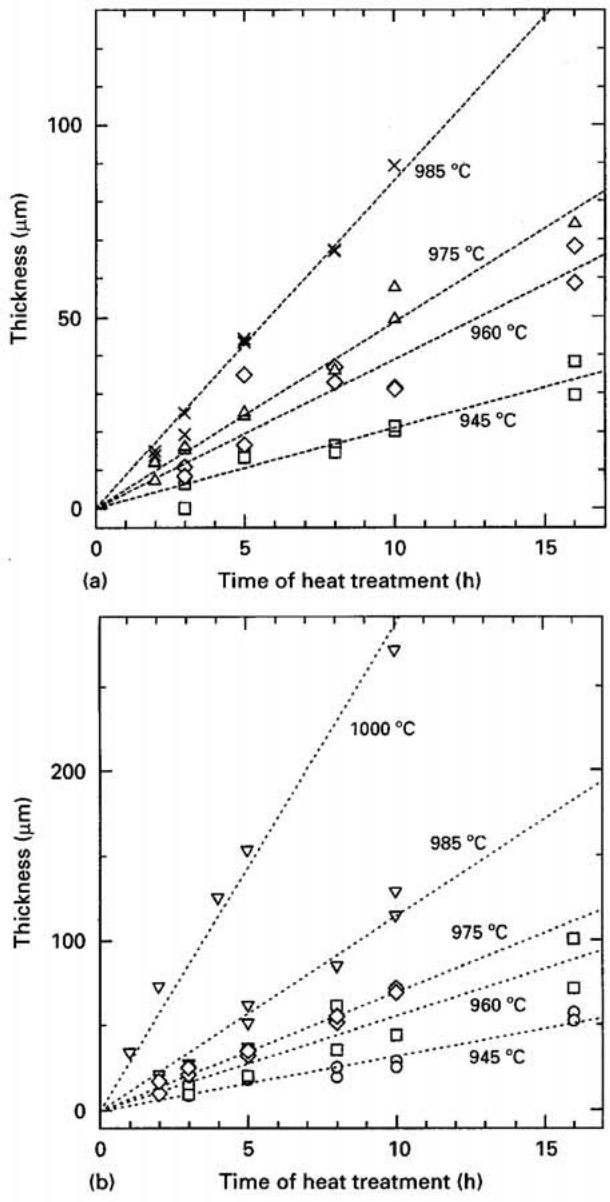

Figure 4 Dependence of growth rates of surface crystals on the temperature of heat treatment: (a) L10, (b) L5N5.

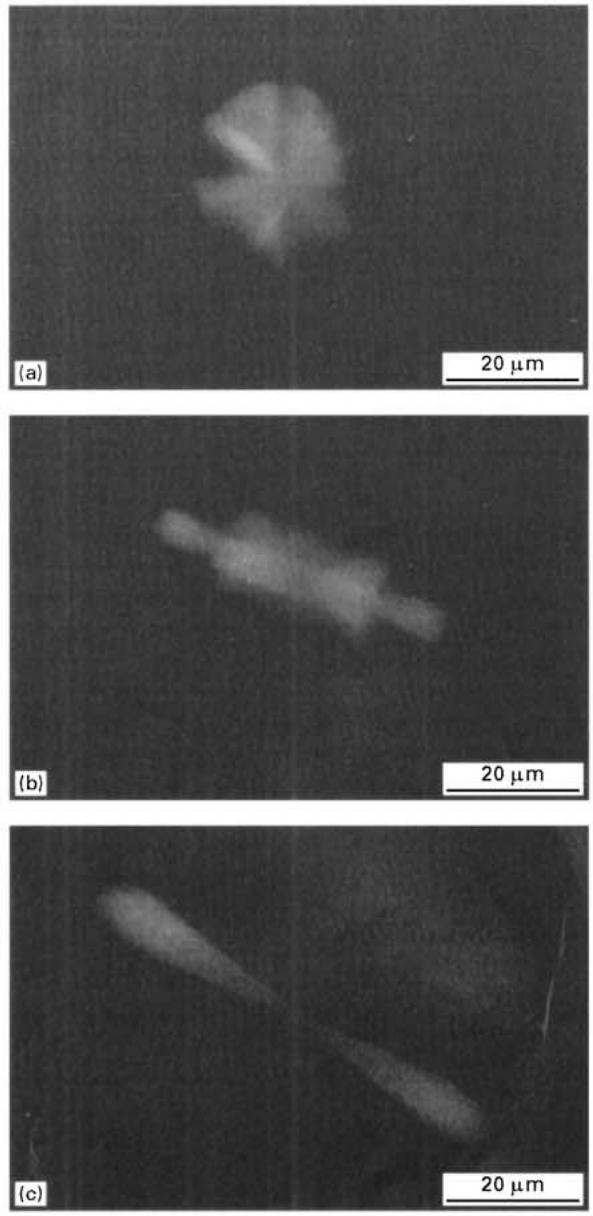

Figure 5 Internal crystals observed by polarizing microscopy. (a) Spherical-shaped crystal in L10 heat treated at 975 °C for 5 h. (b) Stick-shaped crystal in L10 heat treated at 975 °C for 5 h. (c) Stick-shaped crystal in L5N5 heat treated at 960 °C for 5 h.

by 2 mol % Nd_2O_3 (L8N2) and the major phase changed to CNS by substitution of more than 4 mol % Nd_2O_3. Thus, the precipitation of CNS oxyapatite crystals was promoted by the substitution of a small amount of Nd_2O_3 for La_2O_3 in this system.

Fig. 7 shows the micro X-ray diffraction patterns of internal crystals. The stick-like crystals in L5N5 and L10 samples were assigned as CNS and CLS crystals; respectively. However the spherical crystal in the L10 sample was not clearly assigned.

Fig. 8a and b show growth of spherical and stick-like internal crystals in L10 samples and Fig. 8c shows growth of stick-like internal crystals in L5N5 samples. The radius or length of the internal crystals was measured by optical microscopy. Growth rates of crystals showed linearity with respect to time of heat treatment and the neodium-containing sample (L5N5) showed a larger growth rate, as did the surface crystals.

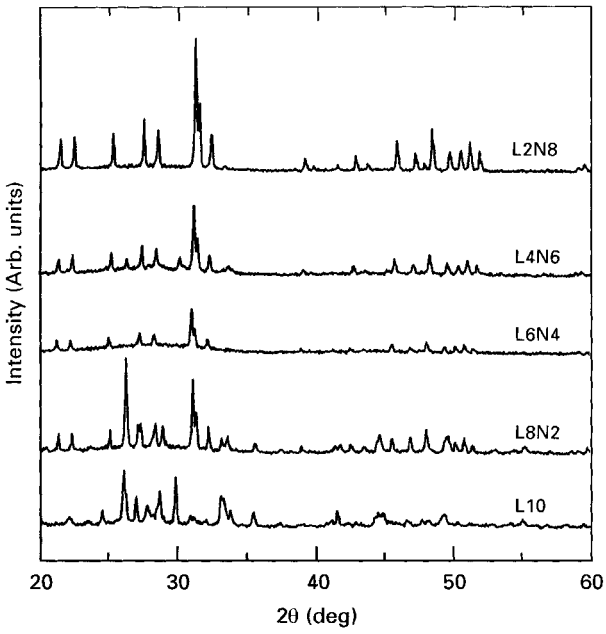

Figure 6 Change in XRD profiles of internal crystals on Nd_2O_3 content.

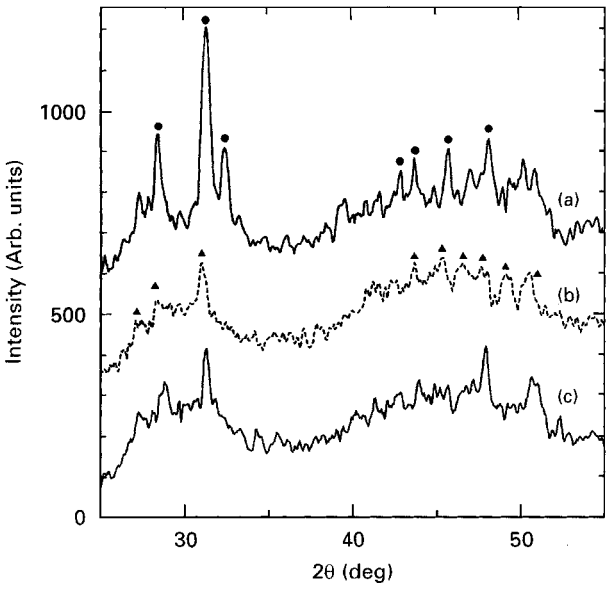

Figure 7 Micro XRD spectrum of internal crystals (heat treated at 975 °C for 10 h). (●) CNS oxyapatite, (▲) CLS oxyapatite.

3.4. Growth rate and apparent activation energy of crystal growth

The apparent activation energies of crystal growth were calculated using the Arrhenius equation $U = A \exp(-E_a/RT)$, where U is the growth rate and E_a is the activation energy. A plot of $\ln U$ versus $1/T$ is shown in Fig. 9. The activation energies estimated from Fig. 9 were 360 kJ mol^{-1} for all surface and internal crystals of this glass. This result is adequate for estimation of the activation energies for crystals which have the oxyapatite structure. Williamson *et al.* [6] reported the activation energy of $30CaO \cdot 2MgO \cdot 15Al_2O_3 \cdot 53SiO_2$ (wt %) glass containing 2.27 and 4.11 wt % V_2O_3 as 243 and 264 kJ mol^{-1}, respectively. The activation energies of glasses of the present

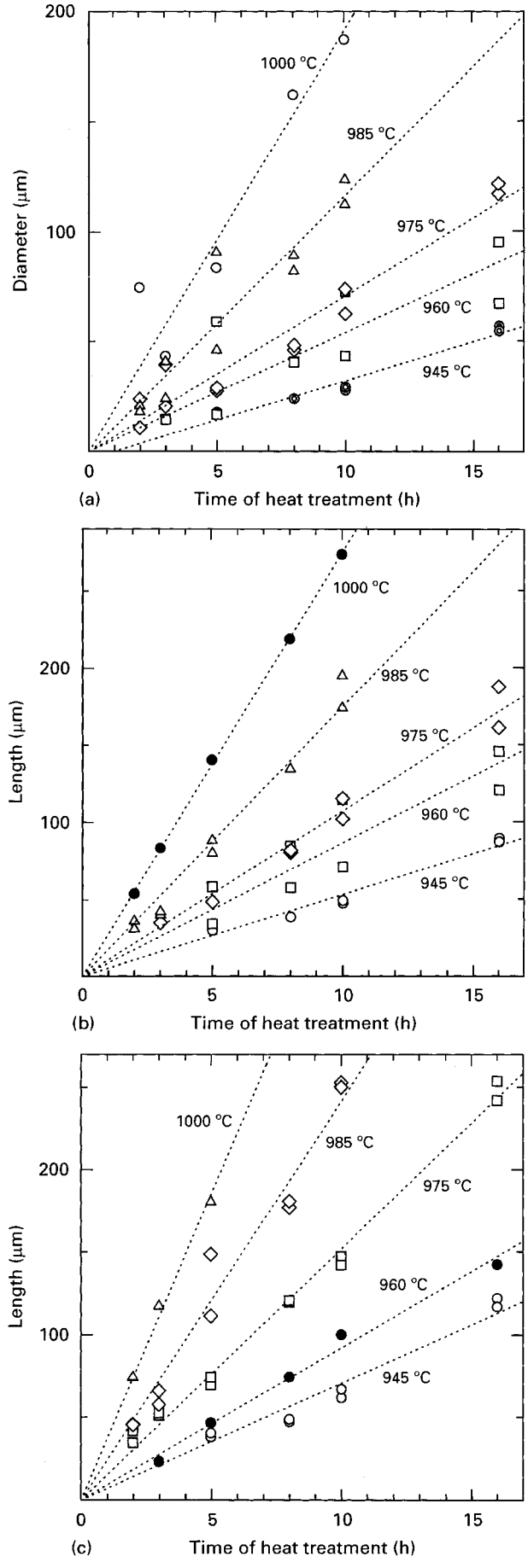

Figure 8 Dependence of growth rates of internal crystals on temperature of heat treatment. (a) Spherical shaped crystal in L10, (b) stick-shaped crystal in L10, (c) stick-shaped crystal in L5N5.

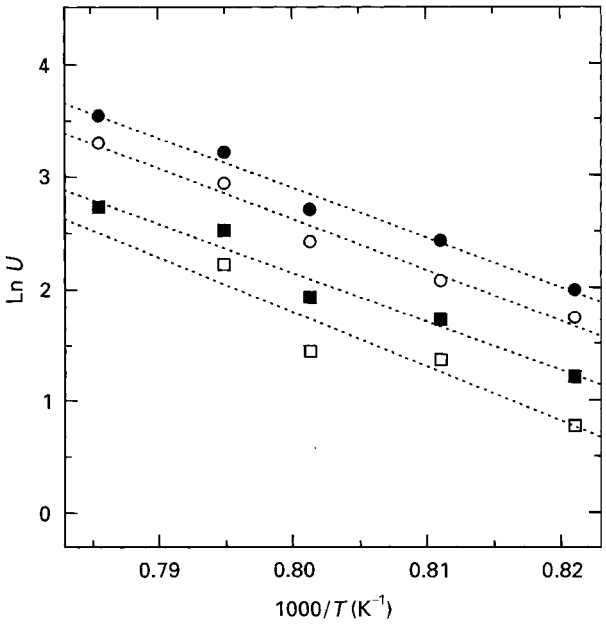

Figure 9 Dependence of growth rates of various crystals (logarithmic values) on reciprocal temperature. U = growth rate (μm). (●) L5N5 (internal), (○) L10 (internal), (■) L5N5 (surface), (□) L10 (surface).

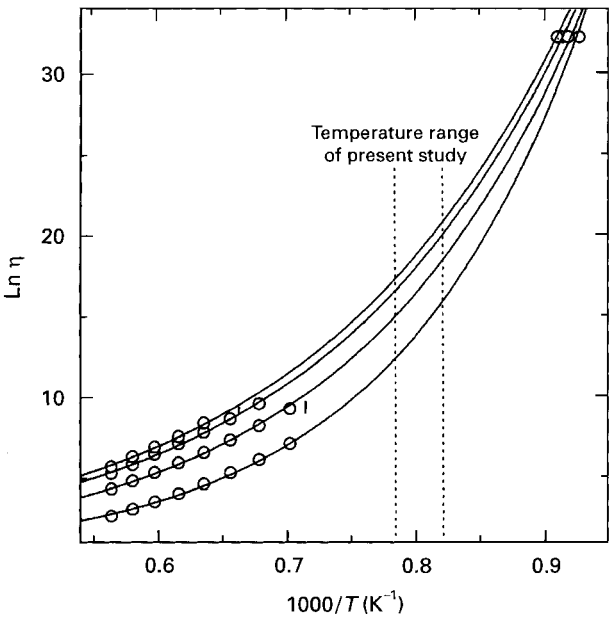

Figure 10 Dependence of viscosity of $CaO–Al_2O_3–SiO_2$ glasses on reciprocal temperature (after [7] pp. 759, 780).

study were higher than in Williamson's study. Figs 10 and 11 show the temperature dependence of viscosity and diffusion constant of $CaO–Al_2O_3–SiO_2$ glasses [7]. In the temperature range of this investigation, the activation energies of viscous flow and diffusion were estimated as 650 and 470 kJ mol^{-1}, respectively. The value of activation energy of crystal growth of $CaO–Al_2O_3–SiO_2–La_2O_3–Nd_2O_3$ glass system (360 kJ mol^{-1}) is closer to that of diffusion than that of viscous flow. Therefore, it is considered that the crystal growth of this glass system is mainly affected by a diffusion process.

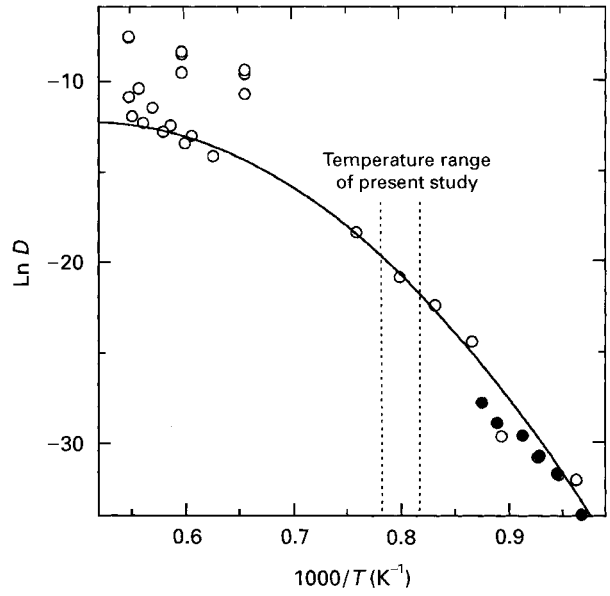

Figure 11 Dependence of diffusion coefficient of (●) Ca^{2+} and (○) O^{2-} in $CaO–Al_2O_3–SiO_2$ glasses on reciprocal temperature (after [7] pp. 858, 860, 861, 866).

4. Conclusion

$CaO–Al_2O_3–SiO_2–La_2O_3–Nd_2O_3$ glasses were prepared and their physical properties and crystallization process were studied. Crystallization of these glasses was observed on the surface and internally within samples. Heat treatment of these glasses precipitated $Ca_2La_8(SiO_4)_6O_2$ oxyapatite (CLS) crystal for $20CaO–10Al_2O_3–60SiO_2–10La_2O_3$ (mol %) glass, and $Ca_2Nd_8(SiO_4)_6O_2$ oxyapatite (CNS) crystal was precipitated on substitution of Nd_2O_3 for La_2O_3. The crystal layer on the surface was clearly observed and the crystals were strongly oriented along the c-axis. Spherical and stick-like internal crystals were observed in $CaO–Al_2O_3–SiO_2–La_2O_3$ glass and stick-like crystals were observed in neodium oxide-containing glass. The stick-like crystals were determined to be CLS or CNS oxyapatite by micro X-ray diffraction.

The apparent activation energies of crystal growth were estimated as 360 kJ mol^{-1} and no dependence on the kind of crystal was observed.

Acknowledgement

This research was supported by a Grant-in-Aid for Scientific Research, The Ministry of Education, Science and Culture, Japan. The authors would like to thank Mac Science Co. Ltd, for micro X-ray diffraction measurement.

References

1. G. H. BEALL, in "Advances in Nucleation and Crystallization in Glass", edited by L. L. Hench and S. W. Freiman (American Ceramic Society, Columbus, OH, 1971) p. 251.
2. D. G. GROSSMAN, *J. Am. Ceram. Soc.* **55** (1972) 446.
3. A. MAKISHIMA, M. KOBAYASHI, T. SHIMOHIRA and T. NAGATA, *ibid.* **65** (1982) C210.

4. A. MAKISHIMA, H. KUBO and T. SHIMOHIRA, *ibid.* **69** (1986) C130.
5. K. MORITA, A. UMEZAWA, S. YAMATO and M. MAKISHIMA, *ibid.* **76** (1993) 1861.
6. J. WILLIAMSON, A. J. TIPPLE and P. S. ROGERS, *J. Mater. Sci.* **4** (1969) 1069.
7. O. V. MAZURIN, M. V. STRELTSINA and T. P. SHAVAIKO-SHVAIKOVSKAYA, "Handbook of glass data, Part C" (Elsevier Science, London 1987).

Received 23 July 1996
and accepted 26 August 1997